Relative Stopping Power of Some Metallic Elements for 28.7-MeV Protons

GEORGE H. NAKANO* AND K. R. MACKENZIE
University of California, Los Angeles, California†

AND

HANS BICHSEL
University of Southern California, Los Angeles, California‡

(Received 8 May 1963)

The stopping power of Be, Ti, V, Co, Ni, Cu, Ag, Ta, W, Ir, and Au were compared with Al at an average proton energy of 28.7 MeV. Accuracies of 0.25% were obtained by using a scattering foil and subsequent collimation to produce two identical beams. The energy and intensity were continually monitored in one beam. Comparisons were made in the other by rotating the samples to produce small changes in thickness. Anomalously high stopping powers were observed in the transition region where the 3*d* shell is being filled inside a completed *s* shell.

INTRODUCTION

RECENT energy-loss measurements on protons below 20 MeV show small deviations from a monotonic trend as a function of Z.[1–4] The anomalies occur in the first series of transition elements from Ca to Ni, with inconclusive suggestions of similar effects in heavier transition regions. The variations are ascribed to a partially filled *d* shell inside a completed *s* shell, and roughly agree with a theory based on changes in electron density.[5]

The present investigation at higher energy was carried out with the proton beam of the USC linear accelerator. Thin samples of Be, Ti, Co, Ni, Cu, Ag, Ta, W, Ir, and Au, were compared with Al at an average energy of 28.7 MeV. The pulses from the Linac were approximately 100 μsec wide and occurred 15 times per sec. Unfortunately, from pulse to pulse, the beam fluctuated as much as 1% in energy and 3 to 5% in intensity. The equipment was designed to cope with these conditions, and comparisons within 0.25% could be made during any period where a train of 10 to 15 satisfactory pulses would follow in succession.

APPARATUS AND PROCEDURE

The measurements were made with two identical beams produced in the manner in Fig. 1. After collimation to 0.08-in. diam, the protons from the Linac were multiply scattered in a 30-mil Mylar foil (scatterer in Fig. 1) and then recollimated by a 0.025-in. vertical slit. The resulting vertical fan of particles was deflected in a 30-deg analyzing magnet, and after traversing a distance of approximately 10 ft from the Mylar foil, was separated by collimator L (see Fig. 1) into two beams 0.05 in. wide by 0.15 in. high, with a vertical separation of 1.5 in. The proton energy was then reduced by aluminum plates, called range adjusters, whose angle with respect to the beam could be set remotely so that the end of the range for each beam occurred in the differential ionization chambers. The upper chamber was used to monitor beam energy and beam current while stopping power comparisons were made in the lower one.

The pulse signals from the current monitors (first plates of ion chambers) were displayed on a dual trace oscilloscope, and were equalized by slight variations in the vertical deflecting magnet at the exit end of the Linac. This controlled the spot where the incident beam struck the Mylar scattering foil. The absolute incident current was controlled at the Linac source, and was kept at approximately 10^{-13} A, just below the point where serious recombination effects occurred in the chamber. All measurements were made with pulses whose equality could be judged visually within 3% by superposing the signals on the dual trace oscilloscope. The appearance of these ionization pulses is shown in Fig. 2(a).

Figure 1 shows the double differential ionization chamber (filled with 3 atm of argon), which is divided into halves by the central common plate, held at -2500 V. The beams are restricted to the center portions of each half by $\frac{1}{8}$-in.-diam holes which remove protons that are scattered at large angles after emerging from the thick range adjusters. The angular acceptance is ± 2 deg. There are three ion chambers, numbered 1, 2, and 3 in each half, formed by collector plates which are 1, 2, and 3 in. in length. The 1-in. plates are the current monitors mentioned earlier. In normal operation the folded Bragg and ionization curves produce a peak inside the last section with a tail extending into the middle section, see Fig. 1(c). When the particle energy is changed, the pulses from these

* Present address: Lockheed Missiles & Space Company, Palo Alto, California.

† Supported in part by the joint program of the office of Naval Research and the U. S. Atomic Energy Commission.
‡ Supported in part by the U. S. Atomic Energy Commission.

[1] D. Wayne Green, John N. Cooper, and James C. Harris, Phys. Rev. **98**, 466 (1955).
[2] C. P. Sonett and K. R. MacKenzie, Phys. Rev. **100**, 734 (1955).
[3] M. Bader, R. E. Pixley, F. S. Mozer, and W. Whaling, Phys. Rev. **103**, 32 (1956).
[4] V. C. Burkig and K. R. MacKenzie, Phys. Rev. **106**, 848 (1957).
[5] Werner Brandt, Phys. Rev. **88**, 1283 (1952), and Nucl. Sci. Ser. Rept. **29**, 56 (1958).

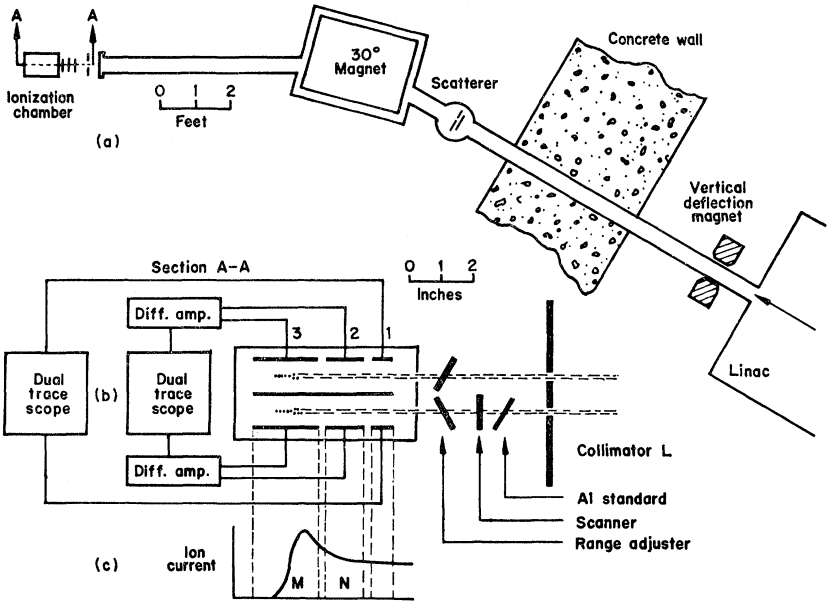

FIG. 1. (a) Plan view of beam trajectory. (b) Side view of differential chambers and foil holders. (c) Location of folded Bragg and straggling curves in the ionization chambers. Areas M and N must be equal for a balanced condition.

sections increase and decrease, respectively, and the difference is a very sensitive function of the change. The ionization pulses from the latter sections in the upper chamber were integrated, with a time constant much longer than the beam pulse length, and compared in a difference amplifier. The resulting signal was displayed on one channel of a dual trace oscilloscope. A null signal could be obtained by correctly setting the angle of the upper range adjuster and the magnetic field in the 30-deg magnet. It was possible to balance the integrated pulses from the two sections, but due to differences in ionization collection times, complete balancing did not occur throughout the pulse duration. Figure 2(b) shows a typical balanced difference signal from the upper chamber with a superposed unbalanced signal from the lower chamber.

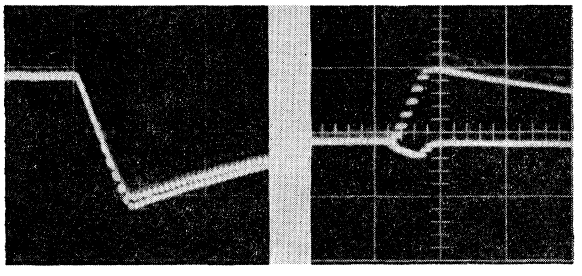

(a) (b)

FIG. 2(a). Superposed pulses from upper and lower current monitors; pulses not quite equal. (b). Differential signals from the upper and lower ionization chambers. The trace from the upper chamber shows the balanced condition with no net vertical displacement at the end of the short Linac pulse. The lack of balance during the pulse is clearly seen. The superposed pulse from the lower chamber is displaced vertically by an amount corresponding to 2% of sample thickness. Chopper amplifiers cause the dotted traces.

Energy-loss comparisons were made in the lower beam. The standard aluminum absorbers were held in a frame which could be remotely rotated through ± 12 deg, indicated in Fig. 1(b). Located immediately behind this frame was the holder for the test samples, called "scanners." Remotely controlled vertical and horizontal motion was provided for this holder so that the test foils could be scanned for nonuniformities.

By stacking several foils, the test absorbers were made thick enough to produce an energy loss very close to 2 MeV. This eliminated the need for a computation of the average beam energy for each foil, and also reduced the number of required Al standards. Except for Be, which was very thick and lapped under oil, the foils were cut as nearly as possible to the same area using a precision die approximately 1 in. square. The edges were clean enough in most cases to permit measurement to 0.0001 in. with a Bausch and Lomb shadow comparator. The individual foils in a test absorber were cleaned with acetone and weighed as a group (usually 2 to 4) on an Ainsworth microbalance to 0.01% or better, using weights recently calibrated at the Bureau of Standards. Buoyancy corrections were applied.

Measurements were made as follows. "Standard" operating conditions were established by adjusting the Linac beam current, the magnetic field in the 30-deg bending magnet, and the angle of the upper range adjuster to produce a null signal from the upper differential chamber. The setting of the upper range adjuster was never adjusted again. A test foil was then inserted into the scanning holder and the angle of the lower range adjuster was set to produce a null from the lower chamber. The intensities in the upper and lower differential chambers were equalized using the vertical

deflecting magnet and the controls for the Linac source. For each new test foil it was necessary to readjust the intensity balance. This was particularly true for the heaviest foils where the intensity in the lower chamber was reduced as much as a factor of 2 by the multiple scattering which deflected many particles outside the 2-deg acceptance angle.

The test foil was scanned for nonuniformity which, if present, was usually in the form of a small uniform taper. Two percent was observed in Ta, and less in other foils. A spot on the foil corresponding to the mean thickness was selected and a null obtained in both upper and lower ionization chambers. The test foil was then removed and an Al standard of 1 to 2% less energy loss was inserted in the rotatable frame and its angle adjusted for a null on both sides of zero. A similar procedure was used for the cross checks which were possible in the few cases where the test samples were close enough in energy loss to permit direct comparisons within the angular limits of the rotatable frame (±12 deg or 2.1% of the Al standard thickness). In spite of infrequent intervals of steady operation an average of 12 measurements were made on each foil.

RESULTS AND DISCUSSION

In Table I the stopping powers of the various materials are compared with that of aluminum. Table II shows the cross checks in which Au and Ag are compared with Cu as the standard absorber. The listed errors are based on a statistical uncertainty of 0.15% in judging the null condition for the test foil and an equal uncertainty for the aluminum standard. Errors in weighing and measuring the foils were of the order of 0.02%. The remainder of the quoted uncertainty is based on an estimate of the error due to nonuniformities. No irregularities were detected in approximately half the foils. Figure 3 shows the relative stopping power per electron plotted against $\ln Z$. The high values of stopping power per electron for Co, V, and Ti confirm the deviation for the transition region reported by earlier authors.

TABLE I. Results of Al comparisons.

Element	Z	Relative mass stopping power S_m	Relative stopping power per electron S_e
Be	4	1.089 ±0.0029	1.1840±0.0032
Ti	22	0.8969±0.0022	0.9409±0.0023
V	23	0.8605±0.0022	0.9185±0.0023
Co	27	0.8501±0.0021	0.8942±0.0022
Ni	28	0.8691±0.0022	0.8780±0.0022
Cu	29	0.8233±0.0020	0.8692±0.0022
Ag	47	0.7164±0.0021	0.7923±0.0023
Ta	73	0.5981±0.0036	0.7143±0.0043
W	74	0.5866±0.0017	0.7023±0.0020
Ir	77	0.5849±0.0017	0.7035±0.0020
Au	79	0.5838±0.0020	0.7014±0.0025

TABLE II. Results of cross checks.

Element	Z	Direct Cu ratio	Calculated Cu ratio from Al comparison
Au	79	0.7071±0.0030	0.7090±0.0028
Ag	47	0.8738±0.0043	0.8701±0.0029

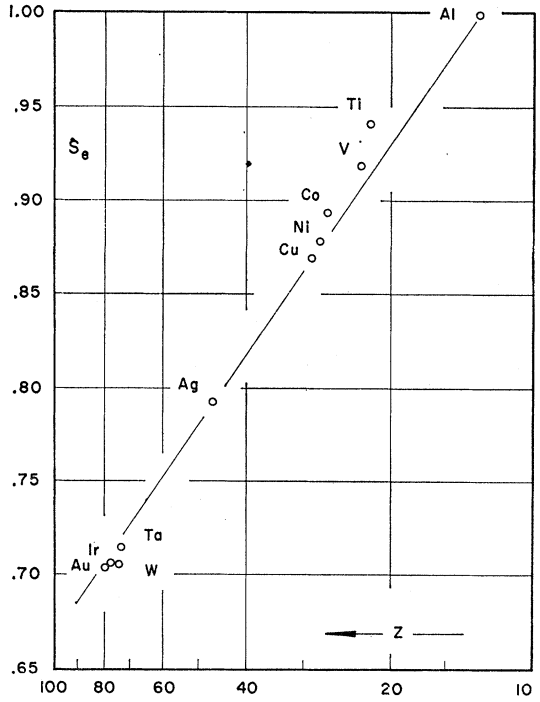

FIG. 3. Relative stopping power per electron versus $\ln Z$.

These measurements of dE/dx were dependent upon an accurate determination of the residual energy of the protons that emerge from the test foil. The good geometry employed in the experiment insured that only protons with an angular deviation of less than 2 deg were used in the measurements. The projected range of such protons closely approximates the true range.

ACKNOWLEDGMENTS

The authors wish to thank Mr. Joel Zuckerman and the USC Linac crew for their assistance, and Professor G. L. Weissler for his encouragement and cooperation in making the USC Linac available for the experiment.

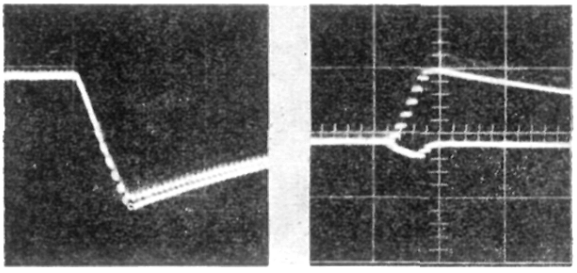

(a) (b)

FIG. 2(a). Superposed pulses from upper and lower current monitors; pulses not quite equal. (b). Differential signals from the upper and lower ionization chambers. The trace from the upper chamber shows the balanced condition with no net vertical displacement at the end of the short Linac pulse. The lack of balance during the pulse is clearly seen. The superposed pulse from the lower chamber is displaced vertically by an amount corresponding to 2% of sample thickness. Chopper amplifiers cause the dotted traces.